

## Behavior of wall panels in industrial buildings caused by differential settlements

Suyai Fernández<sup>1a</sup>, Rossana C. Jaca<sup>2b</sup> and Luis A. Godoy<sup>\*3</sup>

<sup>1</sup>*Intertechne Consultores y Asociados, 8300 Neuquén, Argentina*

<sup>2</sup>*Civil Engineering Department, National University of Comahue, 8300 Neuquén, Argentina*

<sup>3</sup>*Institute for Advanced Studies in Engineering and Technology, IDIT CONICET-UNC, and FCEFyN,  
Universidad Nacional de Córdoba, PO Box 916, 5000 Córdoba, Argentina*

*(Received February 25, 2014, Revised October 20, 2015, Accepted October 28, 2015)*

**Abstract.** This paper presents the analysis of mechanical behavior of metal wall panels of storehouses and industrial buildings subjected to differential settlements. The storehouses considered are representative of those used in the agricultural activity. A small-scale model was built and tested in order to have evidence of the behavior and to validate computational models. The numerical investigation is carried out through finite element analysis using a general-purpose software, by modeling buildings with different geometries and evaluating different settlements of the ground. To obtain an adequate model, geometric non-linearity has to be taken into account. Models that represent the most usual geometric typologies were investigated under support settlements. The deflected shape of the wall panel and the relationship between the horizontal displacements and the settlement of the foundations are evaluated. The results show that there are large out-of-plane displacements caused by settlements that would be admitted by design recommendations.

**Keywords:** buckling; differential settlements; finite elements; industrial buildings; storehouses; wall metal panels

### 1. Introduction

Foundation settlements may induce severe damage in the main resistant structure of industrial buildings and storehouses; further, they can cause damage and induce maintenance issues in secondary structural elements and equipment. Even though structural collapse rarely occurs under support settlements, most of the structural problems associated with poor foundation behavior are linked to settlements which are larger than acceptable values. Criteria for evaluating admissible displacements depend upon the bearing capacity of the soil, but it is also determined by shear at the structural base. The presence of water reduces the load bearing capacity of soils, and this may occur due to seasonal or accidental variations not taken into consideration when structure and foundations design were carried out. Support settlements may also increase with time, so that

---

\*Corresponding author, Professor, E-mail: [luis.godoy@unc.edu.ar](mailto:luis.godoy@unc.edu.ar)

<sup>a</sup>E-mail: [suyaifernandez@yahoo.com.ar](mailto:suyaifernandez@yahoo.com.ar)

<sup>b</sup>Professor, E-mail: [rossana.jaca@fain.uncoma.edu.ar](mailto:rossana.jaca@fain.uncoma.edu.ar)

when the first signs of settlement are identified there is still time to apply corrective measures.

The magnitude of the settlement depends on soil characteristics such as density, voids in soil matrix, size and shape of the grains, degree of soil confinement, soil structure, load history of soil, and characteristics of the applied load. Uniform settlements are not dangerous because the complete structure moves as a rigid body, yet if large differential settlements occur, damage or cracks could appear in the structural components of an industrial building.

This work reports experimental and computational results for small-scale and full-size industrial buildings under differential settlements affecting part of the foundation. The main objective of this research is to explain the basic structural behavior of industrial buildings under settlement, and to quantifying the out-of-plane (horizontal) displacements of the walls as a consequence of vertical displacements at the foundation level.

The problem is motivated by the agricultural activity in the zone of the Alto Valle of Río Negro and Neuquén in Argentina, where numerous storehouses are found. Such facilities are generally located in irrigation areas, where soil may experience an important loss of bearing capacity and produce settlements. As a result of this effect, induced deformations of the wall cladding could cause a loss-of-service condition of the building.

The authors have not been able to identify contributions to this problem in the technical literature, but there are several references addressing structural consequences of settlement for other structural types, such as uneven settlements in shells of revolution, cooling towers, storage tanks, and shallow cylindrical roofs. Jonaidi and Ansourian (1998) investigated the response of thin-walled cylinders under non-axisymmetric, harmonic settlements. Godoy and Sosa (2002, 2003) evaluated the effect of localized support settlements in cylindrical oil storage tanks with a conical roof, using both small-scale models and finite element models of the problem, and found that geometric nonlinearity and buckling are crucial in obtaining credible results. Studies of the same problem in the context of buckling of the shell have been recently reported by Zhao *et al.* (2006), Cao and Zhao (2010), Gong *et al.* (2012, 2013).

Continuous beams with differential settlement were revisited by Sebastian (2010). Settlement at the base of a frame structure has attracted the attention of researchers in the context of buildings. Settlement of plane frame-soil systems was investigated by Agrawal and Hora (2010) under an elastic hyperbolic soil model, and further explored for seismic loads (Agrawal and Hora 2012). Thangaraj and Ilamparuthi (2012) considered frame structures coupled with deformations of the mat foundation. Frame buildings affected by settlement due to soil deformability have been reported by Arapakou and Papadopoulus (2012). Anastasopoulus (2013) recently reported a 5-storey building damage due to a neighboring construction causing differential settlement. The most closely related work to present interest is a case-study of an industrial building performed for a truss structure supported by steel columns (Darmawan 2009).

The research reported in this paper employs a methodology similar to that developed by Sosa and Godoy (2002, 2003): First, a small-scale physical model of an industrial building was tested in a laboratory, in which the descent of one of the support points was induced, measuring the out-of-plane displacements of the walls. Second, a computational model has been made for the same small-scale model to validate the simulation with reference to the physical model. Finally, numerical models of full-scale storehouses representing buildings located in the zone of interest in Argentina are investigated. The models selected have differences in their geometry, in order to consider the effect of different configurations on the structural behavior of the lateral cladding.

This work is part of a more general study on the structural behavior of industrial buildings, and other components of this research program have been recently reported (García-Palencia and

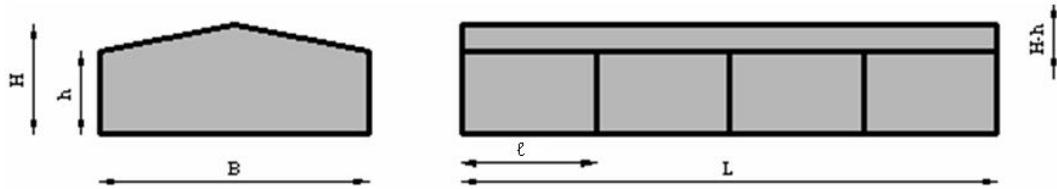


Fig. 1 Nomenclature employed for the storehouse dimensions



(a)



(b)

Fig. 2 Gable roof storehouse with corrugated plate, (a) General view, (b) Internal structure

Godoy 2013, Rosario-Galanes and Godoy 2014).

## 2. Problem characterization

### 2.1 Structural typology

Because this research was motivated by storehouses in Argentina, the first stage was to build an inventory of such structures in the Alto Valle in Río Negro, which is a region of high agricultural (mainly fruit) production in Argentina. This was achieved by visiting establishments and reviewing blueprints of important fruit producers in the area. Geometric information of storehouses were collected as data of interest, using the nomenclature shown in Fig. 1.

In general terms, it can be concluded that: (a) The oldest storehouses have parabolic roof, with more recent constructions having a gable roof. (b) The distance  $\ell$  between frames is virtually the same in all storehouses considered, with values of approximately 5 m. (c) The height  $H$  of ridge level fluctuates between 6 m and 10 m. (d) The height  $h$  of the lateral cladding varies between 4 m and 8m; but in most cases, the height was between 4 m and 6 m. (e) The long side  $L$  of storehouses varies between 20 m and 100 m, of which those with 40 m and 65 m are the most common. (f) The short sides ( $B$ ) of the storehouses have dimensions between 10 m and 50 m, the most common ones being between 25 m and 45 m. (g) The most frequent  $B/L$  ratio is found to be between 0.5 and 0.6.

In the food-storage industries, the new trend in Argentina and elsewhere is to construct storehouses using corrugated plate gable roof and lateral cladding of heat insulating plate panels, as shown in Fig. 2(a). This type of cladding is also commonly employed as new added storehouses



Fig. 3 Gable roof storehouse with sinusoidal plate cladding

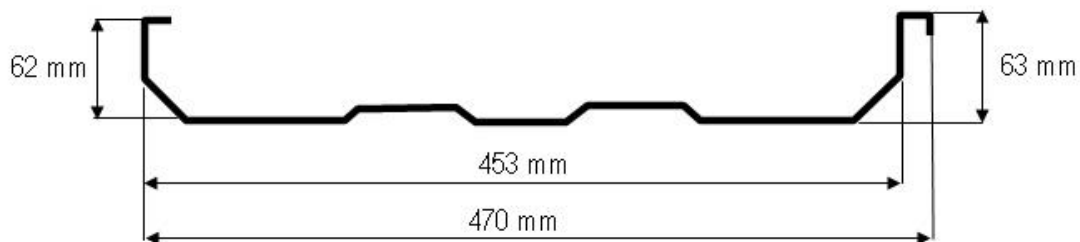


Fig. 4 Panel type U45. Cross Section

by fruit companies that have increased their production capacity. The structure of those more recent buildings are fabricated by means of steel trusses, as shown in Fig. 2(b).

To a lesser extent, there are storehouses with sinusoidal or corrugated plate cladding of the conventional type, as can be seen in Fig. 3, but those are not related to fruit-commercialization activities because they do not provide adequate insulation for frigorific installation.

Based on the data compiled, the present study focused on structures with a regular floor and gable roof, with dimensions representatives of the values found, with type U45 lateral panels covering, as shown in Fig. 4. It is assumed that the steel structures under consideration are hyperstatic and have a superficial foundation.

## 2.2 Recommendations for wall cladding of industrial buildings

Geometric distortions due to large out-of-plane displacements in wall cladding of industrial buildings may affect service conditions, such as the effective use of the structure (doors should open without difficulties), malfunctioning of the machinery attached to the structure (cranes), and its appearance. In high season of fruit production, the rigorous demand of international commerce requires the optimal functioning of cooling systems, because any minor issue could lead to significant economic losses. For this reason, it is important to take preventive measures such as considering the service conditions at the design stage of the project. Considering that panel deformation may provoke loss of isolation to the cold store, then limits to deformations should be stringent.

The Argentinian recommendations for steel structures (CIRSOC 301 2000) establish limitations on total displacement for isolated structural components, such as columns or crane runway beams, by limiting vertical deformations and horizontal displacements to values of  $\ell/150$ , where  $\ell$  is the distance between frames. However, it does not establish limit values for displacements of wall cladding. The recommendation for flexible cladding elements in Argentina (CIRSOC 303 1991),

whose reach includes thin walled cold formed steel structures, does not specify support settlements under cladding. Other recommendations (AISC 2004, ASCE 2002) indicate that the service limit should be set depending on the activity that will be developed in the building. The ASCE recommendation indicates values of maximum displacement between  $H/400$  and  $H/600$ ,  $H$  being the height of the building (ASCE 2002). Given the need to preserve the normal functioning of the fruit conservation system, a maximum horizontal deflection  $H/600$  seems to be an adequate limit and will be considered in this work as a reference value to understand the significance of this problem.

### 2.3 On soil settlements

A settlement may be caused by static or dynamic loads, or by changes in the moisture content due to seasonal fluctuations. Soil deformations leading to vertical settlements are considered in this work, in which the vertical settlement ( $\delta_v$ ) may be written as

$$\delta_v = \delta_i + \delta_c + \delta_f \quad (1)$$

where  $\delta_i$  is the instantaneous settlement;  $\delta_c$  is the primary consolidation settlement; and  $\delta_f$  is the secondary compression settlement (creep settlement).  $\delta_i$  is produced simultaneously with the application of load, and is caused by a reduction of voids. In granulated soils, this effect is dominant.  $\delta_c$  is produced by water expulsion through the soil pores as a function of time. This effect, which is typical of clay, induces volumetric changes of the soil; granular soils, on the other hand, do not usually cause differential settlements due to their high permeability.  $\delta_f$  is produced by changes of shape in the particles that constitute the soil, and could be neglected because it does not produce significant values.

Support settlements are not necessarily related to heavy structures but could also occur in light-weight structures, in which the most damaging effect is the differential settlement of supports. Very flexible structures, such as storehouses, do not have the capacity to redistribute loads thorough other load transfer mechanisms, and consequences of differential settlements may be severe. An angular distortion  $\beta$  is often employed in the form

$$\beta = \frac{\delta_v}{\ell} \quad (2)$$

The most common criteria for limiting angular distortions are: (a)  $\beta=1/500$  to avoid cracking; (b)  $\beta=1/300$  if cracking is expected in walls; (c)  $\beta=1/150$  inadmissible cracks and damage affecting structural elements.

To establish limits according to rational recommendations, maximum values of 20 mm to 25 mm to support settlements are frequently established for granular soils, and 40 mm to 50 mm for cohesive soils.

## 3. Analysis of a small-scale model

### 3.1 Experimental model

A small-scale physical model has been fabricated, in which the main structure is represented by

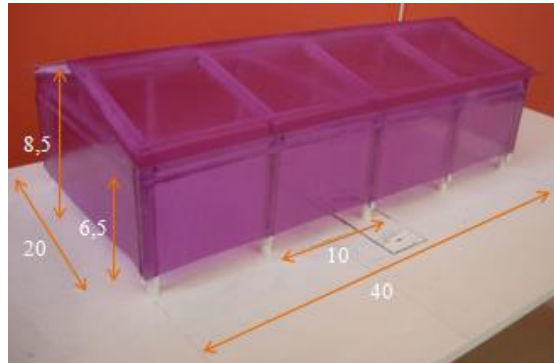


Fig. 5 Small-scale physical model, dimensions in cm



(a)



(b)

Fig. 6 General viewpoint of physical model, (a) Measuring device, (b) Device to impose vertical descents in the central column

wood bars and cladding is formed by acetate sheets. The columns are clamped at the base, with the exception of one of the main columns, in which a 2 mm settlement is induced by means of a mechanism that simulates differential soil settlement. Out-of-plane displacements of one of the walls adjacent to the affected column are measured. A dimensional analysis has not been used for the tests, because testing in this case seeks to identify the qualitative behavior of the structural system including modes and amplitudes of deflections. The purpose of testing a small-scale model is twofold: First, to visualize and quantify the expected out-of-plane displacements; second, to serve as benchmark for validation of finite element models.

The dimensions of the model in plan are  $B=200$  mm wide and a length  $L=400$  mm, with a separation between frames  $\ell=100$  mm. The ridge height is  $H=85$  mm and the height of the metallic cladding is  $h=65$  mm. The finished model is shown in Fig. 5, where the central column can



Fig. 7 Front view of the deformation in physical model due to differential settlement of central column ( $\delta_{vmax}=2$  mm)

descend due a manufactured groove on the table. In a 1:50 scale, the model represents a 10 m×20 m storehouse, with a ceiling height of 3 m minimum and a maximum height of 4 m.

Fig. 6(a) shows a measuring device, consisting of a digital caliber (with precision 0.005 mm), placed over a Bunsen support. A hole was drilled on the supporting table, close to the central column, to impose the vertical displacement through the device shown in Fig. 6(b). A grid was placed on the acetate sheet, to locate the points where measurements are taken and to be able to link them with the computational mesh. Tests were conducted to evaluate the mechanical parameters of acetate, resulting in elastic modulus  $E=3,000$  MPa and Poisson ratio  $\nu=0.4$ .

Fig. 7 shows a front view of the deformation in the acetate sheet due to a vertical displacement of 2 mm of the central column in the experimental model. In the same figure one can also observe the points in which displacements are measured, which are separated 8mm amongst themselves.

### 3.2 Finite element analysis of the small-scale model

A computational model has been performed with the same dimensions and material parameters used in the experimental model. Due to symmetry of the problem, only half of the structure has been discretized.

Modeling by finite elements is done by means of the general-purpose code ABAQUS (2006), in which the wall and roof cladding are discretized with four-node quadrilateral shell elements identified as S4R, with five degrees-of-freedom per node. Based on observations of the physical model and a modeling of half of the structure, the influence of support settlement extends through the shell up to the next frame and is negligible beyond it. For this reason, part of the structure between two consecutive frames is represented in the model, where one is the central frame (to which symmetry conditions are imposed) and the other frame has boundaries conditions corresponding to the joint between the plate and the frame, shown in Fig. 8. Riks algorithm (1972, 1979) was used to obtain nonlinear static equilibrium solutions to unstable problems, in which the load and/or displacement decrease along the path.

Fig. 9(a) shows the part of the structure considered in the model, representing a sector between two successive frames, as described in Fig. 8. Columns of the physical model located at the end of the sector studied are represented by means of restrictions of the translational and two rotational degrees-of-freedom, allowing rotation of the plate around the column, in three columns designated

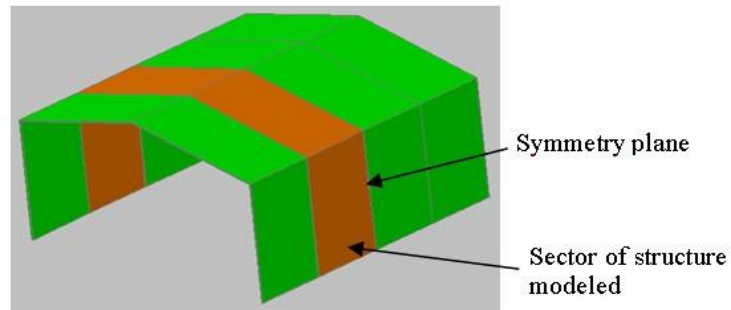


Fig. 8 Part of storehouse considered in computational model

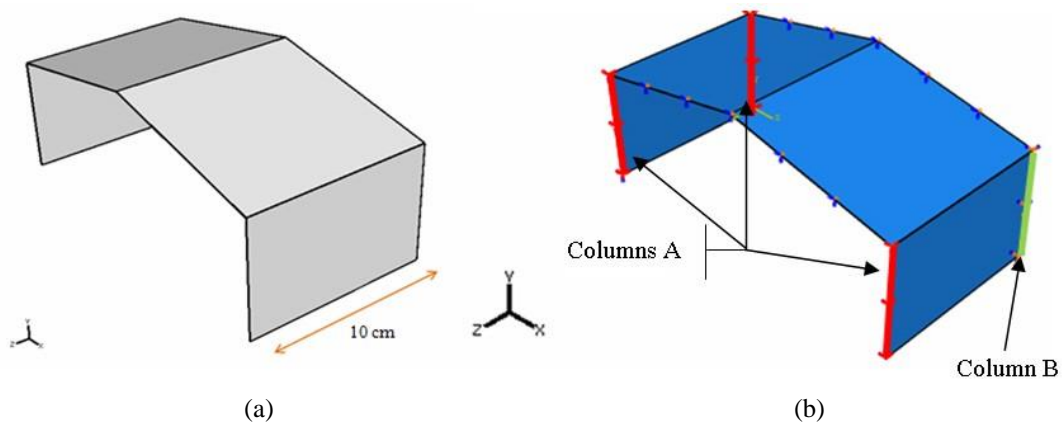


Fig. 9 Numerical model, (a) Sector of structure modeled, (b) Boundary conditions

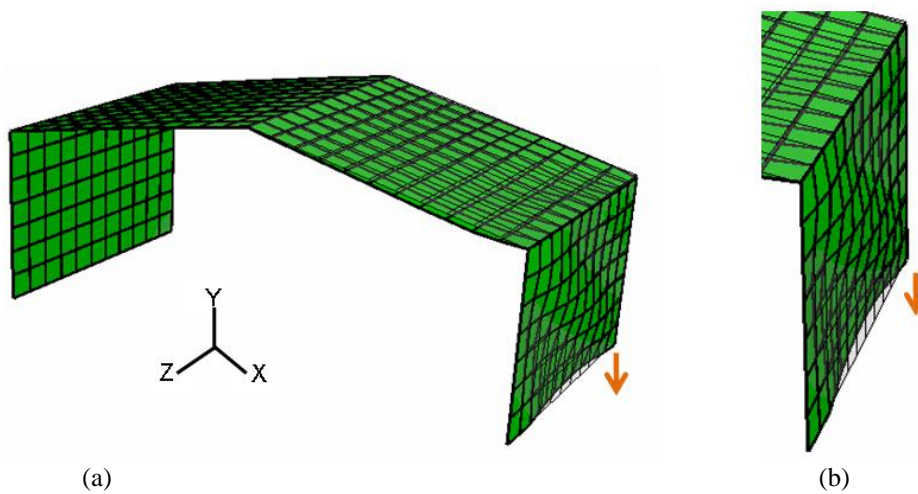


Fig. 10 Deformed numerical model, (a) General viewpoint, (b) Near viewpoint

as *A* (see Fig. 9(b)). In the fourth column (*B*) located at the planes of symmetry, a 2 mm settlement is imposed, as was done in the physical model. Convergence analyses were carried out to define

the element mesh, so that a relative error does not exceed 1%.

The behavior of the material is assumed to be linear elastic because the acetate of the plate does not reach plasticity under the applied stresses. Although some orthotropy has been detected in the tests conducted to this material (ASTM 2000), the difference between both directions is small; for that reason, the material is simulated as isotropic with  $E=3,000$  MPa and  $\nu=0.4$ .

Geometrically linear analysis does not provide satisfactory results because it does not approximate the results in the physical model, resulting in a numerical deformation considerably different from that observed in the model. It was found necessary to employ geometrically nonlinear analysis (GNA). Godoy and Sosa (2002) found similar results when evaluating the response of small-scale tanks when under localized settlement.

In agreement with the test conducted in the physical model, a vertical settlement of 2 mm is applied to one of the plate vertical boundaries and out-of-plane displacements are computed, as shown in Fig. 10. The displacement contours that result from the numerical modeling are shown in detail in Fig. 11, representing the out-of-plane displacements in the plates (U1) with a maximum displacement of 2.9 mm. Negative values of U1 represent displacements towards the inside of the storehouse.

Fig. 12 shows the deformation of the physical and computational models, and it can be seen that both models lead to qualitatively similar results. For conducting a quantitative validation, it is vital to measure the vertical displacements in different areas of the physical model where changes take place; this is indicated in Fig. 13 with a square, in relation to the reference system shown in that same figure. In terms of the coordinated axis shown in Fig. 13, cross-sections are seen along the Z-axis, in which the results for both models are shown. Fig. 14 presents the results for measurements along with numerical values in different sections along the Z-axis, where the out-of-plane displacements (U1) are shown at different elevation of the storehouse (according to the Y-axis).

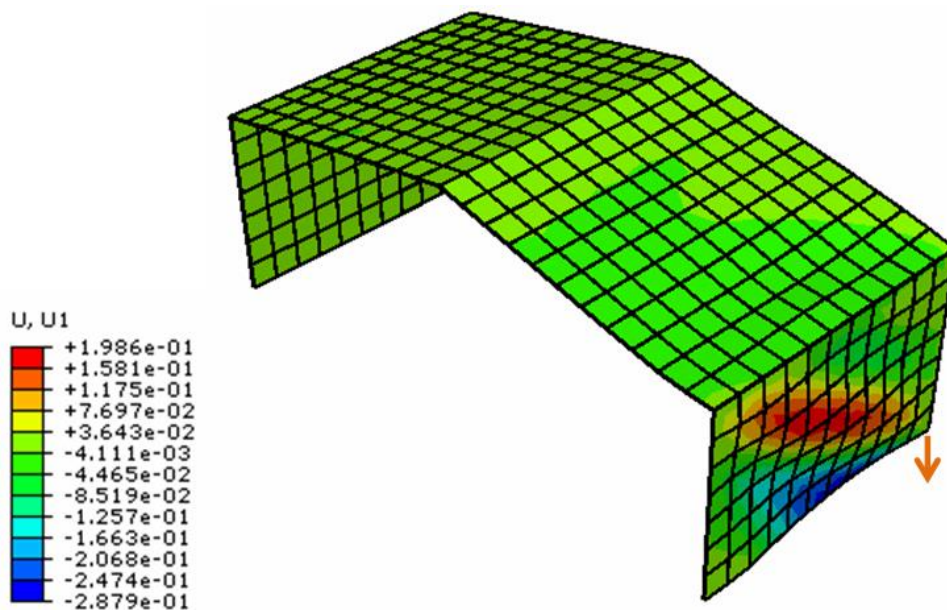


Fig. 11 Out-of-plane displacements in the plates (U1), in cm

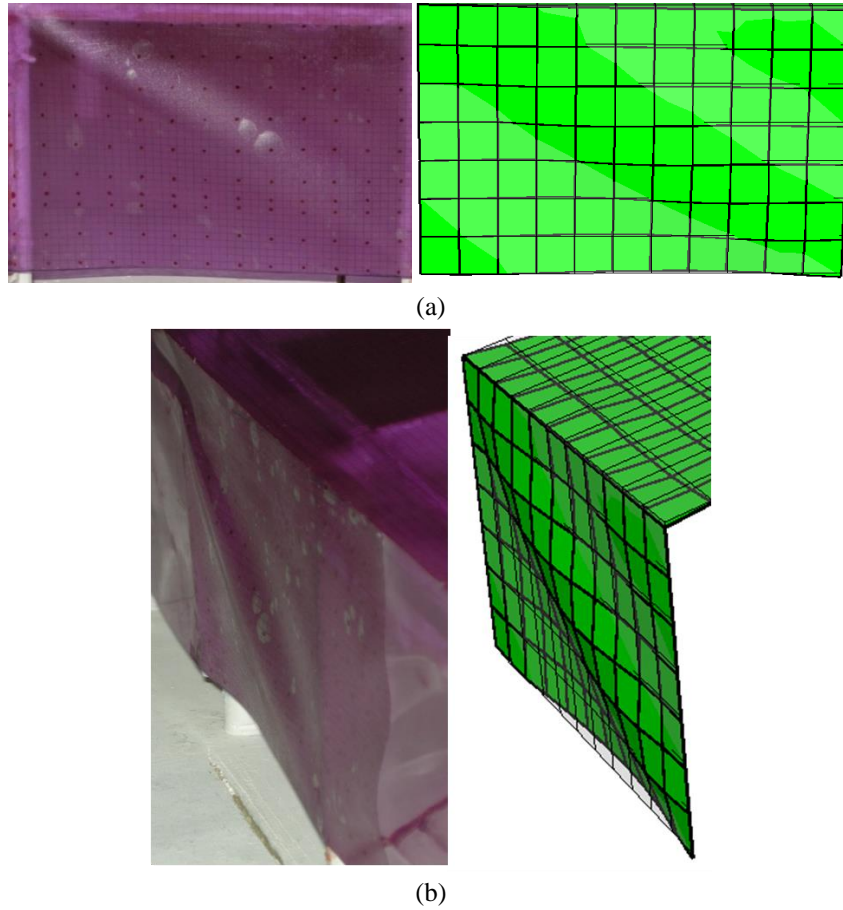


Fig. 12 Comparison between physical and computational models, (a) Front view, (b) Lateral view

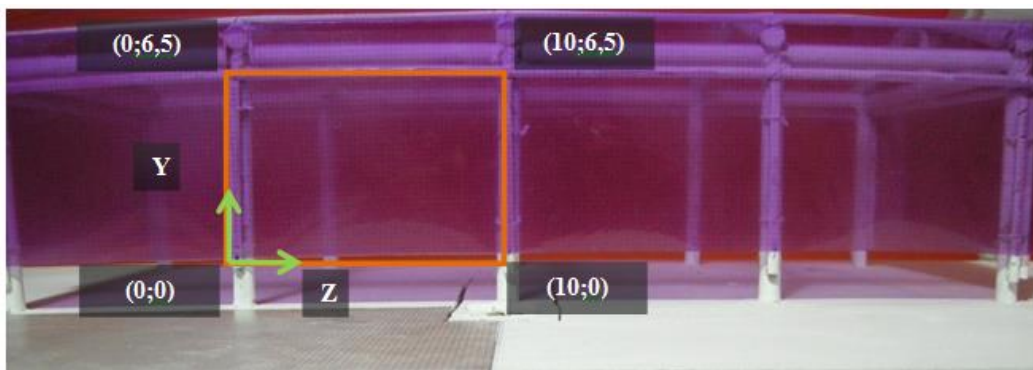


Fig. 13 Reference system for result comparison, coordinates expressed in cm

Good agreement can be seen between the values obtained in the physical model and those obtained in the computational model, both quantitatively and qualitatively. The numerical model captures the deformation pattern exhibited in the plates of the physical model.

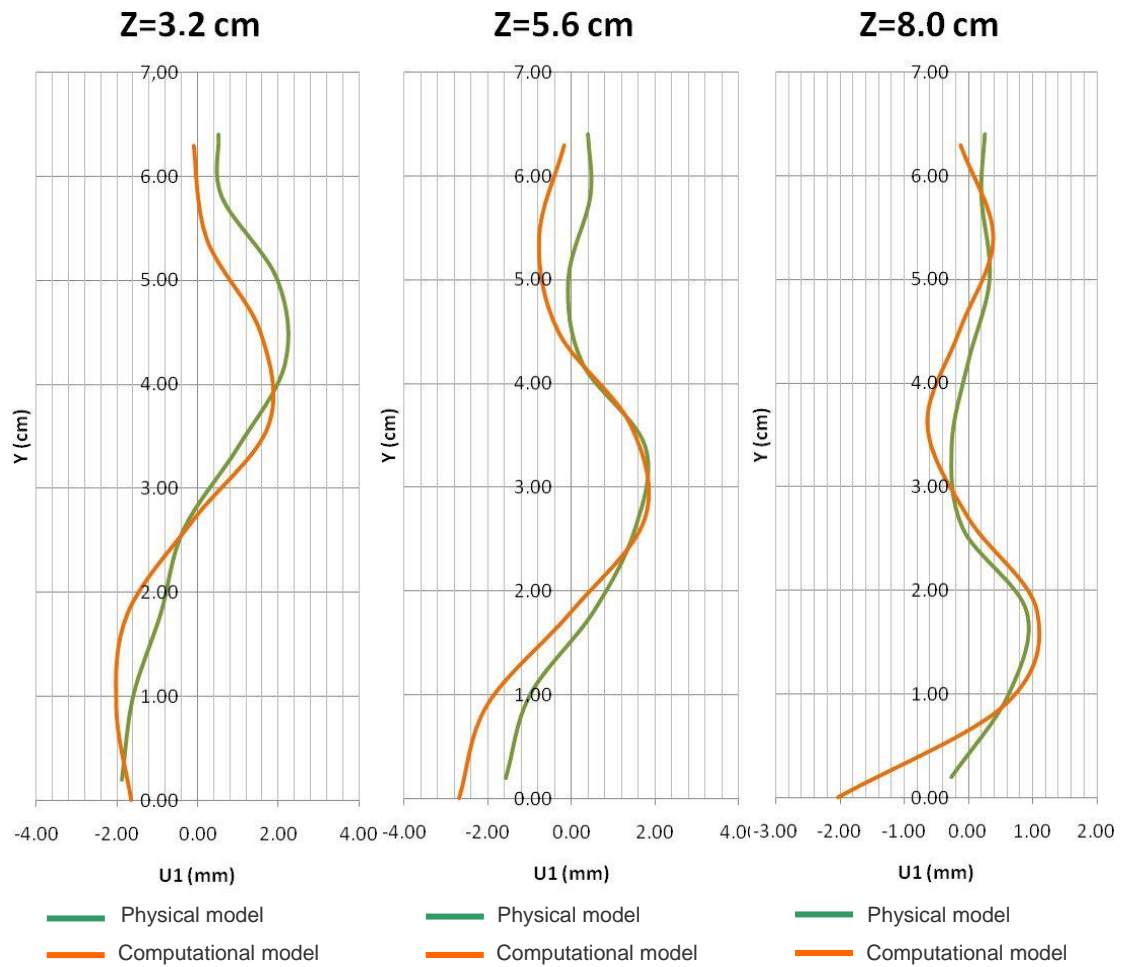


Fig. 14 Comparison between experimental and computational out-of-plane displacements, for  $Z=3.2$  cm,  $Z=5.6$  cm and  $Z=8.0$  cm

Table 1 Geometry of computational models

Model	$H$ (m)	$h$ (m)	$\ell$ (m)	$B$ (m)	$\delta_v$ (mm)
M1	6	4	5	20 and 45	5 to 25
M2	7	5	5	20 and 45	5 to 25
M3	8	6	5	20, 25, 30, 45 and 50	5 to 25
M4	9	7	5	20 and 45	5 to 25
M5	10	8	5	20 and 45	5 to 25

#### 4. Analysis of full-scale store houses

To investigate the structural behavior of industrial buildings subjected to a support settlement, a series of storehouse models were investigated in real scale using finite elements, introducing

variations in the geometrical parameters.

Modeling full-scale industrial buildings is also done by means of a geometrically nonlinear analysis, GNA. Different models listed in Table 1 were studied by imposing a vertical displacement  $\delta_v$  at the central support. Industrial buildings with gable roof are represented because they are the most commonly used in recent constructions, as was previously mentioned. The most representative dimensions of the existing industrial buildings were considered, based in the compiled inventory in the region.

Cladding is composed of corrugated carbon steel plates of low alloy, fabricated through cold-forming process. This partition is represented in the model with a rectangular section plate of 0.5 mm thickness, in this way its strength is equivalent to that of the corrugated plate. Elastic parameters  $E=202$  GPa and  $\nu=0.3$  have been assumed.

The soil is not modeled in this study, but it is assumed as a boundary condition, in which there is a vertical displacement of one of the columns. The magnitude of displacement is variable in each model, but has a maximum value of 250 mm, in agreement with the limits proposed by technical recommendations.

This model seeks to determine the behavioral pattern of cladding in industrial buildings under a vertical support displacement and to compare the maximum out-of-plane displacements with the admissible values specified in the regulations that attempt to protect the service conditions.

Five cases were investigated: Figs. 15 to 19 show the results for models M1, M2, M3, M4, and M5, all with a  $B=20$  m width and a variable height of the lateral walls ranging between  $h=4$  m and

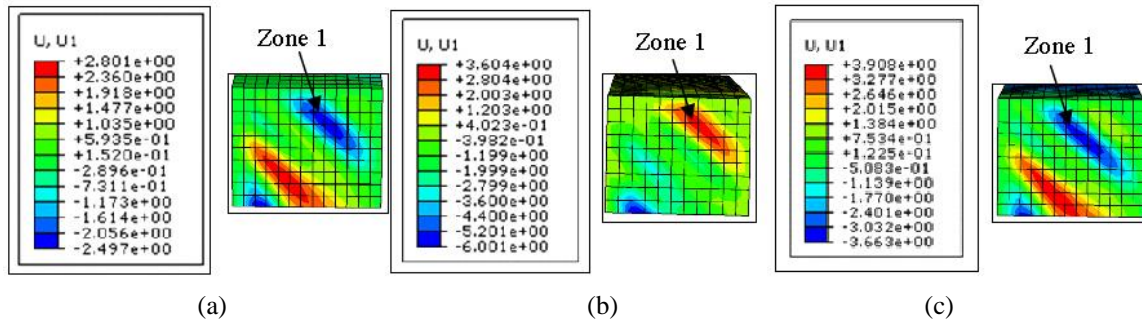


Fig. 15 Out-of-plane displacements for model M1 ( $B=20$  m,  $h=4$  m), in cm, (a)  $\delta_v=5$  mm, (b)  $\delta_v=9$  mm, (c)  $\delta_v=10$  mm

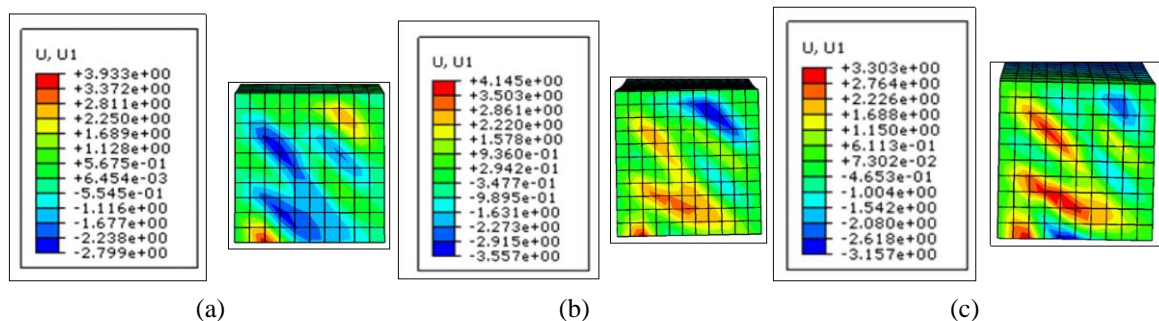


Fig. 16 Out-of-plane displacements for model M2 ( $B=20$  m,  $h=5$  m), in cm, (a)  $\delta_v=7$  mm, (b)  $\delta_v=9$  mm, (c)  $\delta_v=10$  mm

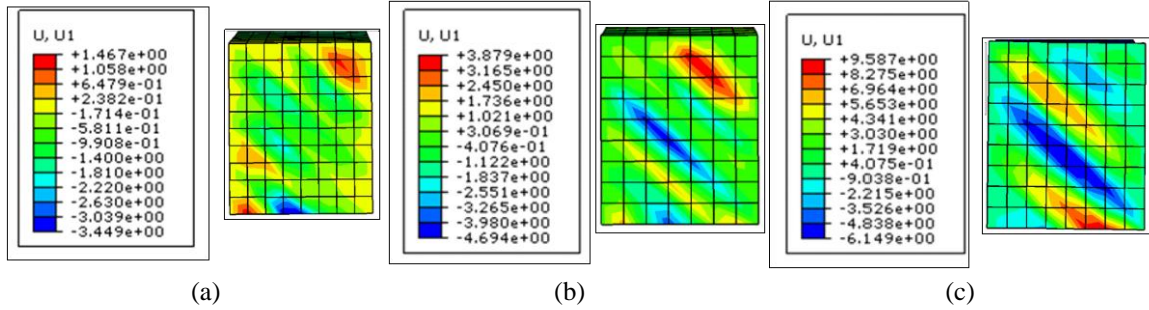


Fig. 17 Out-of-plane displacements for model M3 ( $B=20$  m,  $h=6$  m), in cm, (a)  $\delta_v=5$  mm, (b)  $\delta_v=10$  mm, (c)  $\delta_v=25$  mm

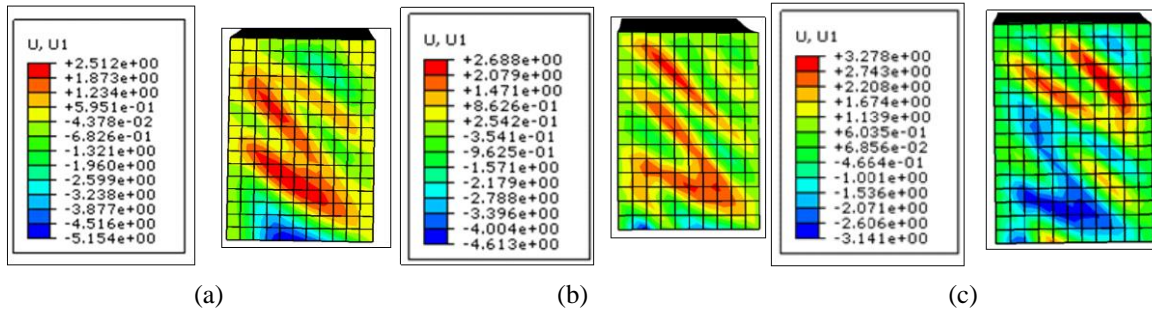


Fig. 18 Out-of-plane displacements for model M4 ( $B=20$  m,  $h=7$  m), in cm, (a)  $\delta_v=5$  mm, (b)  $\delta_v=9$  mm, (c)  $\delta_v=10$  mm

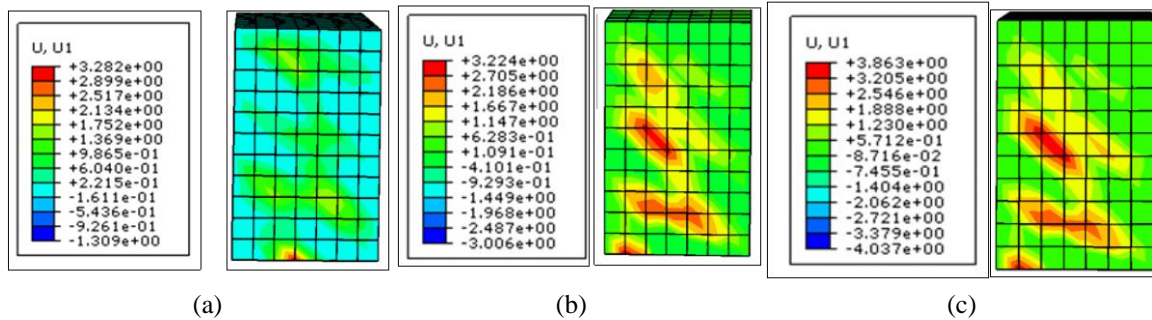


Fig. 19 Out-of-plane displacements for model M5 ( $B=20$  m,  $h=8$  m), in cm, (a)  $\delta_v=5$  mm, (b)  $\delta_v=7$  mm, (c)  $\delta_v=10$  mm

$h=8$  m, with variable support settlements between 5 mm and 25 mm. Fig. 20 shows a comparison of industrial buildings with a width  $B=45$  m; 5 m and 6 m height; and 10 mm settlement.

The results show a trend in deflected patterns of inclined bands, in agreement with the distortion obtained in the physical model. This similarity is more evident in Figs. 15 to 18 (for  $0.8 \leq h/\xi \leq 1.2$ ), where a pattern of inclined bands at approximately  $45^\circ$  may be observed. Figs. 18 and 19 show higher  $h$  values, but their patterns of deformation are not as evident as in the shorter cases.

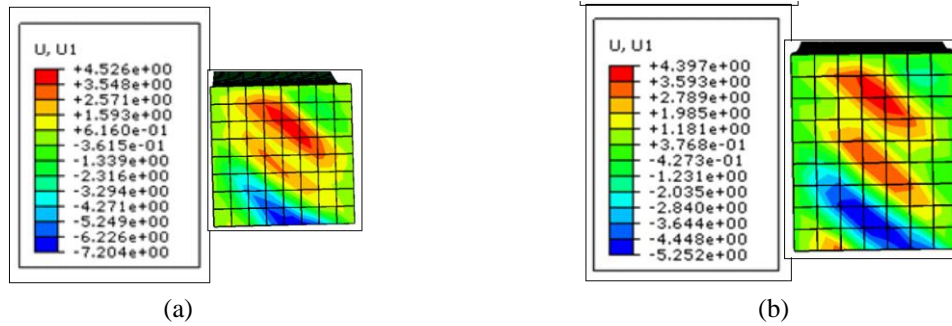


Fig. 20 Comparison between models M2 y M3 ( $B=45$  m,  $\delta_v=10$  mm), in cm, (a)  $h=5$  m, (b)  $h=6$  m

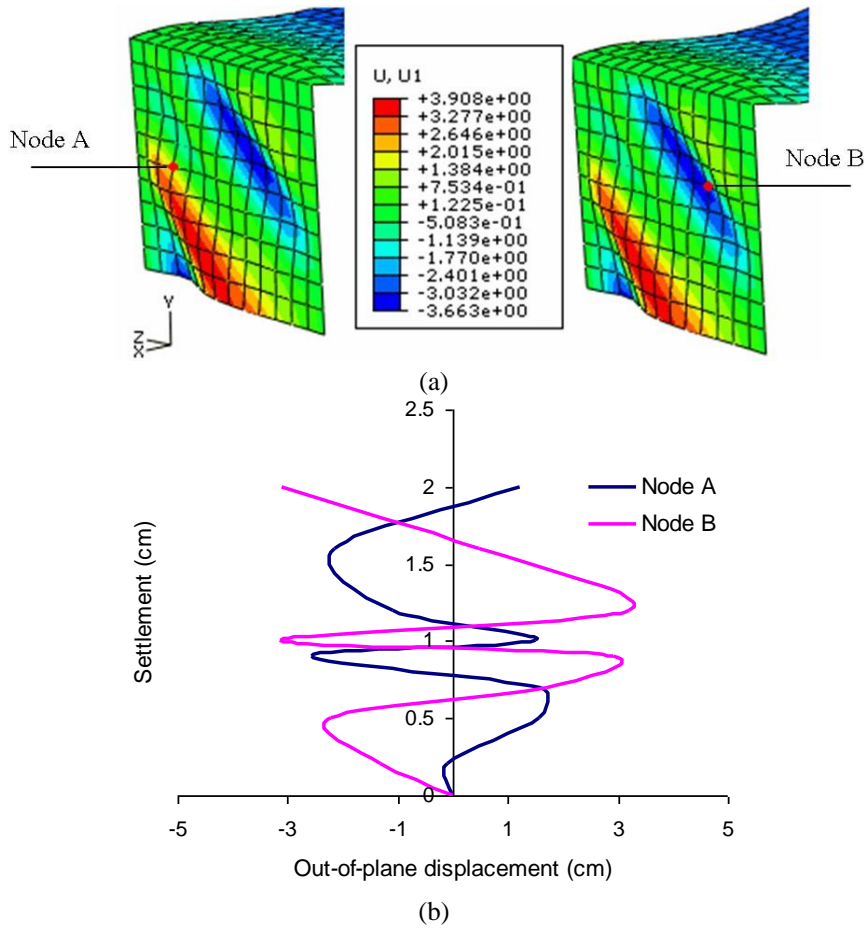


Fig. 21 Model M1 ( $B=20$  m,  $h=4$  m), (a) Location of nodes investigated ( $\delta_v=10$  mm), (b) Equilibrium paths for the nodes investigated

In all the cases studied in this paper, an increase in the magnitude of the out-of-plane displacements of the plate occur as the vertical in-plane settlement increases.

Figs. 15(a)-(b)-(c) correspond to support settlements that increase from 5 mm to 10 mm and it

can be seen that the zones of deformation are modified from the inside of the storehouse to the outside, with a snap-through behavior. Moreover, variations of maximum out-of-plane displacements are not aligned with the settlement. The values of U1 in the upper section of the plate (zone 1) are: 25 mm for  $\delta_v=5$  mm and 36 mm for  $\delta_v=9$  mm and  $\delta_v=10$  mm. In the rest of the cases one can observe an analogue pattern to that in Fig. 15, in other words, there is a nonlinear behavior.

Considering the models with the same settlement ( $\delta_v=10$  mm) and with equal width of the construction ( $B=20$  m), but with different values of  $h$ , it can be seen that there are values of U1 between 33 mm and 47 mm. Nevertheless, it is not possible to find a clear pattern of behavior with the variation of  $h$ , because it produces a distinct deflected shape. Specifically, Fig. 20 shows the deformations for storehouses with the same width ( $B=45$  m) and variable height ( $h$ ) for a single settlement  $\delta_v=10$  mm, similar to previous analysis. In this case, the behavioral pattern is similar and the maximum values are somewhat higher for a smaller height.

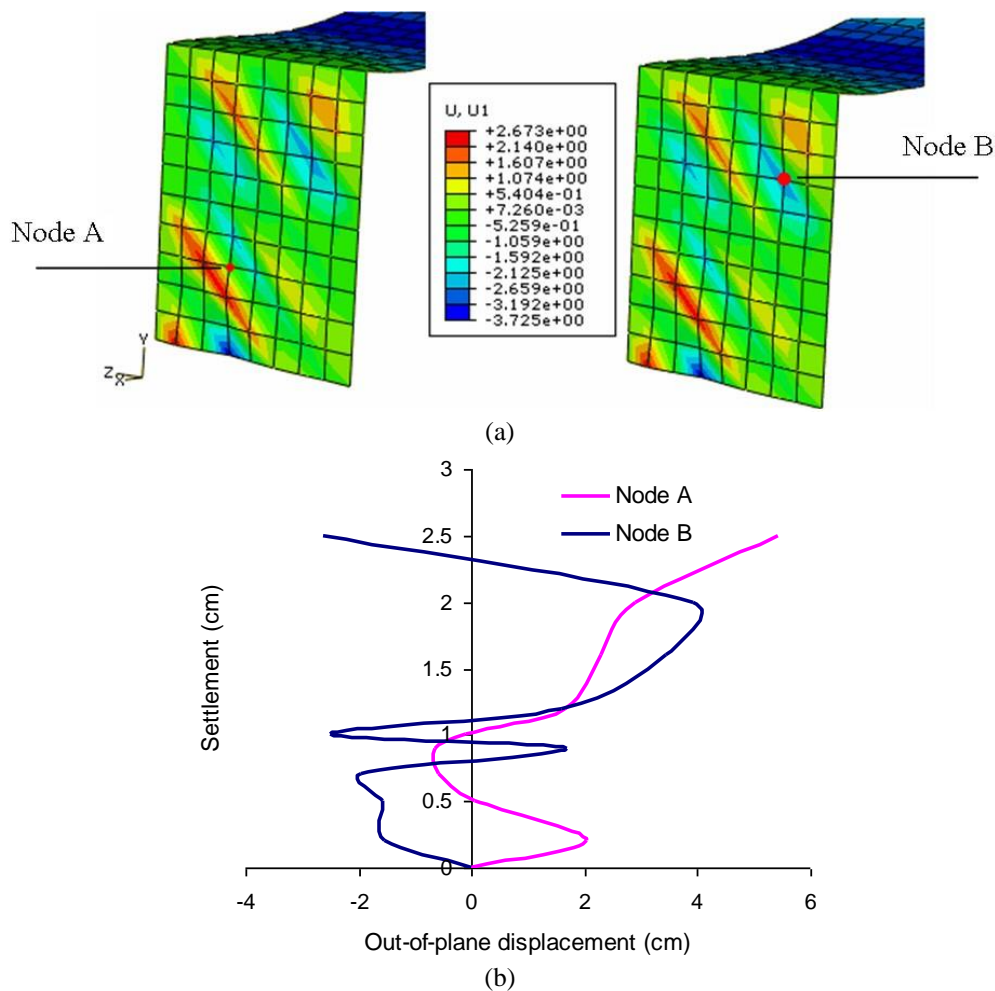


Fig. 22 Model M3 ( $B=20$  m,  $h=6$  m), (a) Location of nodes investigated ( $\delta_v=10$  mm), (b) Equilibrium paths for the nodes investigated

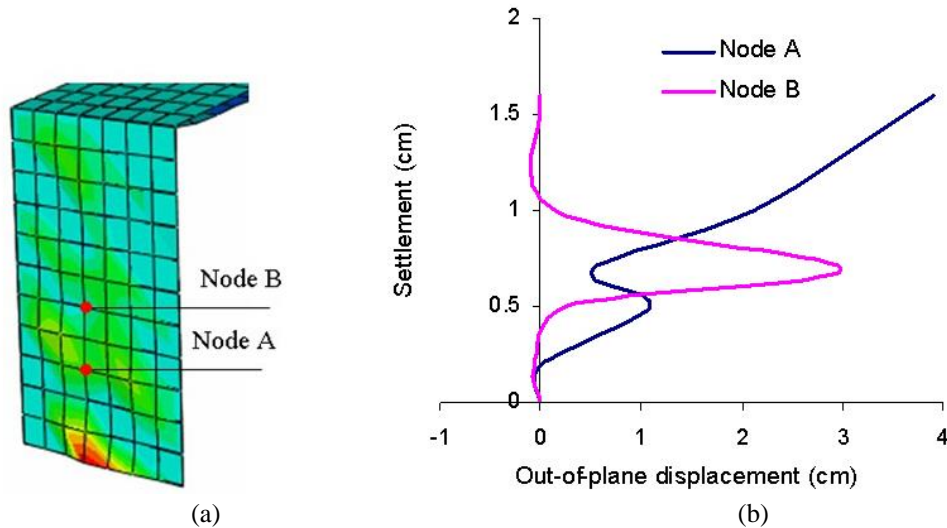


Fig. 23 Model M5 ( $B=20$  m,  $h=8$  m), (a) Location of nodes investigated ( $\delta_v=10$  mm), (b) Equilibrium paths for the nodes investigated

Using one of the industrial buildings as a reference case, that which has the highest value of  $H=10$  m, the maximum admissible value given by ASCE (2002) is

$$\frac{H}{600} = 1.67\text{cm} \quad (3)$$

This value is exceeded in all models considered in this research, for applied settlements lower than the admissible values.

Results of geometrically non-linear analysis are presented in Fig. 21 in terms of out-of-plane displacements as a function of increasing vertical displacements for the Model identified as M1. Equilibrium paths are shown for two nodes, identified as A and B, located in zones where the largest displacements are computed (see Fig. 15). Out-of-plane displacements of increasing amplitude are obtained, which alternatively change from outwards to inwards. Thus, mode changes are experienced along the non-linear equilibrium path.

For Models M3 and M5, in which the width  $B$  of the building is constant and the height of the metal shell is changed, equilibrium paths are shown in Fig. 22 for M3 at points A and B for increasing settlement amplitude. The behavior is similar to what was observed in the previous case, with alternating inwards and outwards displacements in shear bands; those increase with settlement amplitude. Results for Model M5 having a larger value of  $h$  are shown in Fig. 23, there is also the formation of a shear band but with a different pattern dominated by outward displacements.

## 5. Conclusions

This work has presented the response of structural systems of industrial storehouses with gable roof subject to differential settlement in its supports, with a special emphasis on the behavior of

out-of-plane displacements to the walls. Computational models have been used to represent the problem, and comparisons between a small-scale physical and finite element models have been made.

The results show that in order to obtain adequate representation of the structural response, it is crucial to include geometrical non-linearity as part of the model. The modeling of a sector of the industrial nave, by use of symmetry conditions, leading to a simple model provides results in agreement with the physical model. The comparison between physical and numerical model for a small-scale model was acceptable and allowed identification of the non-linear behavior. The finite element methodology has next been employed to analyze full-scale structures and obtain conclusions on their behavior.

The results indicate that the influence of the support settlement is extended from the shell all the way up to the consecutive frame and from that point on the effect is negligible.

From the computational models, it can be concluded that:

- The deflected pattern is formed in general by 45° shear bands which alternate storehouse displacements inside and out.
- There is a direct non-linear relationship between the differential settlements in the soil and the maximum perpendicular deflections to the plane of lateral flexible cladding.
- For different relations between the frame height and the distance among frames,  $h/\ell$ , the distorted shape of cladding changes, which makes it difficult to identify a deformation pattern as a function of the variation of this parameter. For the same  $h/\ell$  relation and different descents, the distortion does not produce damage, but the amplitudes of the out-of-plane displacements change.
- Not all features of an industrial building have been modeled in this work. Many industrial buildings have additional stiffening of the walls which are not included in this research.
- The different values for  $B$  affect the lateral cladding response, although it was not possible to determine a behavior pattern for this parameter.

## Acknowledgments

This work was supported by grants from Universidad Nacional del Comahue, Universidad Nacional de Córdoba, and CONICET.

## References

- ABAQUS (2006), ABAQUS User's Manuals Version 6.3, Hibbitt, Karlsson and Sorensen, Inc. Rhode Island, USA.
- Agrawal, R. and Hora, M.S. (2010), "Effect of differential settlements on nonlinear interaction behaviour of plane frame-soil system", *ARPJ. Eng. Appl. Sci.*, **5**(7), 75-87.
- Agrawal, R. and Hora, M.S. (2012), "Nonlinear interaction behaviour of plane frame-layered soil system subjected to seismic loading", *Struct. Eng. Mech.*, **41**(6), 711-734.
- AISC (2004), *Serviceability Design Considerations for Steel Buildings*, American Institute of Steel Construction, USA.
- Anastasopoulos, I. (2013), "Building damage during nearby construction: Forensic analysis", *Eng. Fail. Anal.*, **34**, 252-267.
- Arapakou, A.E. and Papadopoulos, V.P. (2012), "Factors affecting differential settlements of framed structures", *Geotech. Geol. Eng.*, **30**(6), 1323-1333.

- ASCE (2002), *Minimum Design Loads for Buildings and Other Structures*, American Society of Civil Engineers, USA.
- ASTM D882-02 (2002), *Standard Test Method for Tensile Properties of Thin Plastic Sheeting*, American Section of the International Association for Testing Materials, USA.
- Cao, Q.S. and Zhao, Y. (2010), "Buckling strength of cylindrical steel tanks under harmonic settlement", *Thin Wall. Struct.*, **48**(6), 391-400.
- CIRSOC 301 (2000), *Reglamento Argentino de Estructuras de Acero para Edificios*, Centro de Investigación de los Reglamentos Nacionales de Seguridad para Obras Civiles, Buenos Aires.
- CIRSOC 303 (1991), *Estructuras Livianas de Acero*, Centro de Investigación de los Reglamentos Nacionales de Seguridad para Obras Civiles, Buenos Aires.
- Darmawan, M.S. (2009), "A case-study of structural assessment of steel structure subjected to differential settlement of foundation", *1st International Conference on Rehabilitation and Maintenance in Civil Engineering (ICRMCE)*, Solo, Indonesia, 312-320.
- García-Palencia, A.J. and Godoy, L.A. (2013), "Fatigue experiments on folded plate steel cladding under wind", *Struct. Eng. Mech.*, **46**(3), 387-402.
- Godoy, L.A. and Sosa, E.M. (2002), "Deflections of thin-walled storage tanks with roof due to localized support settlement", *Proc. II Int. Conf. on Advances in Structural Engineering and Mechanics*, Techno Press, Seoul, Korea.
- Godoy, L.A. and Sosa, E.M. (2003), "Localized support settlements of thin-walled storage tanks", *Thin Wall. Struct.*, **41**, 941-955.
- Gong, J., Cui, W. and Zeng, S. (2012), "Buckling analysis of large scale oil tanks with a conical roof subjected to harmonic settlement", *Thin Wall. Struct.*, **52**(7), 143-148.
- Gong, J., Tao, J., Zhao, J., Zeng, S. and Jin T. (2013), "Effect of top stiffening rings of open top tanks on critical harmonic settlement", *Thin Wall. Struct.*, **65**, 62-71.
- Gong, J., Tao, J., Zhao, J., Zeng, S. and Jin, T. (2013), "Buckling analysis of open top tanks subjected to harmonic settlement", *Thin Wall. Struct.*, **63**, 37-43.
- Gong, J., Zeng, S. and Jin, T. (2013), "Effect of hydrostatic pressure on buckling behavior of storage tanks under local support settlement", *ASME Pressure Vessels and Piping Conf., Design and Analysis*, **3**, Paris, France.
- Jonaiddi, M. and Ansourian, P. (1998), "Harmonic settlement effects on uniform and tapered tank shells", *Thin Wall. Struct.*, **31**, 237-255.
- Riks, E. (1979), "An incremental approach to the solution of snapping and buckling problems", *Int. J. Solid. Struct.*, **15**, 529-551.
- Riks, E. (1972), "The application of Newton's method to the problem of elastic stability", *J. Appl. Mech.*, **39**, 1060-1065.
- Rosario-Galanes, O. and Godoy, L.A. (2014), "Modeling of wind-induced fatigue of cold-formed steel sheet panels", *Struct. Eng. Mech.*, **49**(2), 237-259.
- Sebastian, W.M. (2010), "Criteria for uniqueness and extrema of moments in continuous end spans with differential settlement", *Eng. Struct.*, **32**, 1568-1576.
- Thangaraj, D.D. and Ilamparuthi, K. (2012), "Numerical analyses of soil-mat foundation and space frame system", *Int. Multis. Mech.*, **5**(3), 267-285.
- Zhao, Y., Cao, Q.S. and Xie, X.Y. (2006), "Floating roof steel tanks under harmonic settlement: FE parametric study and design criterion", *Journal of Zhejiang University, Science A*, **7**(3), 398-406.